A human-inspired mechanical criterion for multi-contact locomotion in humanoids

F. Bailly[1,2,†], J. Carpentier[1,2], B. Pinet[1], P. Souères[1], B. Watier[1,2]

***Abstract*— This work aims at experimentally identifying a mechanical principle of locomotion stability in humans and demonstrating that this principle can be used for generating stable multi-contact motions for humanoids. For this purpose, a destabilizing setup was built on which five different experiments were carried out by 15 human volunteers. We first show experimentally that when humans balance is perturbed (walking on a destabilizing setup, increasing walking speed, grasping or not a fixed element), the distance between the center of mass (CoM) and the central axis of the external contact wrench significantly increases. This result is coupled with a theoretical reasoning in mechanics in order to exhibit how lowering this distance amounts to lower the body's angular acceleration and thus constitutes a good strategy against falling. Finally, we illustrate the interest of this result for humanoid robot motion generation by embedding the minimization of the distance between the CoM and the central axis of the external contact wrench in an optimal control formulation in order generate multi-contact locomotion.**

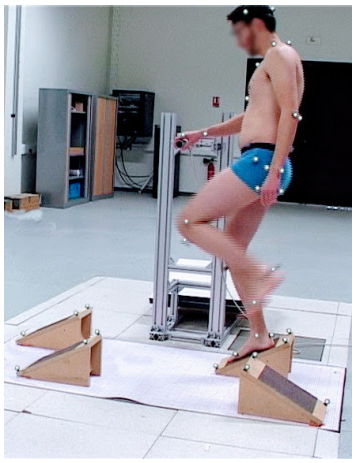

Fig. 1: Overview of the experimental setup during a recording session. A participant is asked to walk through a destabilizing setup while using the handlebar to help himself.

I. Introduction

A. Motivations

Stability of human locomotion embodies a scientific challenge related to both humanoid robotics and biomechanics. Researchers have widely used the Zero Moment Point (ZMP) to evaluate the degree of stability during locomotion on horizontal walkways [1]. The ZMP is the intersection of the locomotion plane and the axis along which the moment of contact forces under the feet is collinear to the normal of the plane.

Several authors have suggested that locomotion becomes unstable when the ZMP is close to the boundary of the support polygon [2]. This criterion has been widely used in biomechanics, to investigate gait control analysis, running mechanics, prosthesis, shoes design and fall detection [3], [4]. In these approaches, the authors have usually studied the ZMP trajectory during several tasks, which is considered to reflect information about neuromuscular control [5].

In robotics, researchers have also used ZMP control to generate bipedal locomotion trajectories [2]. However, this criterion suffers from limitations as it is only defined when contacts are coplanar. Thus, this criterion becomes irrelevant when motions involve multiple non-coplanar contacts while this situation is common in everyday life (stairs climbing, door opening, elderly locomotion ...) and increasingly used in humanoid robotics trajectory generation [6], [7].

To overcome these limitations, several works have been proposed to expand the ZMP criterion when locomotion is performed on uneven surfaces or when bipeds use multi-contacts (cane, banister, etc.). Using a barycentric method weighted by contact surfaces slopes and forces applied at each foot, the computation of a virtual contact surface from which the ZMP could be calculated was suggested in [1]. In [8], authors have proposed to compute a generalized ZMP inside a virtual surface obtained by projecting the edges of the convex hull of the supporting contact points onto the floor. In [9], it was proposed that if the CoM of the biped was inside the polyhedral convex cone of the external contact wrench between the feet of a biped and its environment, its balance is assured. The geometrical complexity of all these propositions makes them poorly intuitive for expressing a generalized criterion that might be used as a sensorimotor strategy for gait or locomotion balance control in humans.

B. Outline of the paper

In this paper, we propose a study of locomotion stability based on a mechanical approach. This work is built on the computation of the external contact wrench (see Sec. II). The key idea is to consider the central axis of this wrench along which the moment of the contact forces applied to the body and the resultant of the contact forces are collinear. This axis is known as the set of points where the overall moment induced by contact forces is minimal for the Euclidean norm (see Sec. II), and can always be computed even for generalized locomotion (uneven surfaces or multi contacts).

[1]LAAS-CNRS, 7 Avenue du Colonel Roche, F-31400 Toulouse, France
[2]University of Toulouse, UPS, LAAS, F-31400 Toulouse, France
[†]Corresponding author (fbailly@laas.fr)

The overall moment applied to the CoM is also, according to Euler's second law, the variation of angular momentum at the CoM, and thus reflects the body's angular acceleration. Within the scope of bipedal locomotion, being balanced meaning not to fall or not to tumble, it is then intuitive to minimize this quantity. This can be the consequence of minimizing the distance between the CoM and central axis of the external contact wrench.

Hence, we propose to analyse this distance during destabilized locomotion. After having theoretically demonstrated the consistency of this reasoning, we present the results of experimental tests in humans (see Sec. III). We hypothesize that this distance should significantly become greater under increasingly perturbed balance conditions. This conjecture is corroborated by setting up walking experiments to study five different locomotion tasks involving non-coplanar and contacts with upper limbs. This result is then applied in the context of multi-contact locomotion of humanoid robots (see Sec. IV). This is done by including the distance between the CoM and the central axis of the external contact wrench in the cost function to be minimized within our trajectory generation framework [10]. The simulation results performed with the model of HRP-2 show that minimizing this distance under appropriate constraints leads to dynamically consistent and whole body feasible centroidal trajectories. These results also support that our criterion generalizes previously proposed practices for handling the derivative of angular momentum in humanoid trajectory generation by being less conservative and more versatile.

II. Mathematical background

Notations. In the sequel, G is the global CoM, Δ is the central axis of external contact wrench and $d_{G-\Delta}$ is the distance between G and Δ.

Contact forces can be represented by a single vector $\mathbf{f}$. At any point A, $\mathbf{f}$ induces a moment $\mathbf{m_A}$. $\mathbf{f}$ and $\mathbf{m_A}$ define a moment field (that we call external contact wrench) that is expressed at any point B as:

$$\mathbf{m_B} = \mathbf{m_A} + \mathbf{f} \times \overrightarrow{\mathbf{AB}} \tag{1}$$

where vector $\overrightarrow{\mathbf{AB}}$ gives the position of B with respect to A. It is well known that there exists one axis such that, at each point of this axis, the moment is parallel to $\mathbf{f}$ [11]. This axis, directed by $\mathbf{f}$, is the central axis of the external contact wrench (Δ). Without loss of generality, assuming that $A \in \Delta$, and taking the Euclidean norm of (1) yields:

$$||\mathbf{m_B}||_2^2 = ||\mathbf{m_A}||_2^2 + ||\mathbf{f} \times \overrightarrow{\mathbf{AB}}||_2^2 + 2\, \mathbf{m_B} \cdot (\mathbf{f} \times \overrightarrow{\mathbf{AB}}) \tag{2}$$

with $2\, \mathbf{m_A} \cdot (\mathbf{f} \times \overrightarrow{\mathbf{AB}}) = 0$ (hypothetically the moment about A is parallel to $\mathbf{f}$). This leads to the conclusion that, at any point B, $||\mathbf{m_B}||_2^2 \geq ||\mathbf{m_A}||_2^2$, reaching the equality when B belongs to Δ. Δ is computed thanks to [12]:

$$\forall B \text{ in space},\ \forall A \in \Delta,\ \overrightarrow{\mathbf{BA}} = \frac{\mathbf{f} \times \mathbf{m_B}}{||\mathbf{f}||^2} + \lambda \mathbf{f},\ \lambda \in \mathbb{R} \tag{3}$$

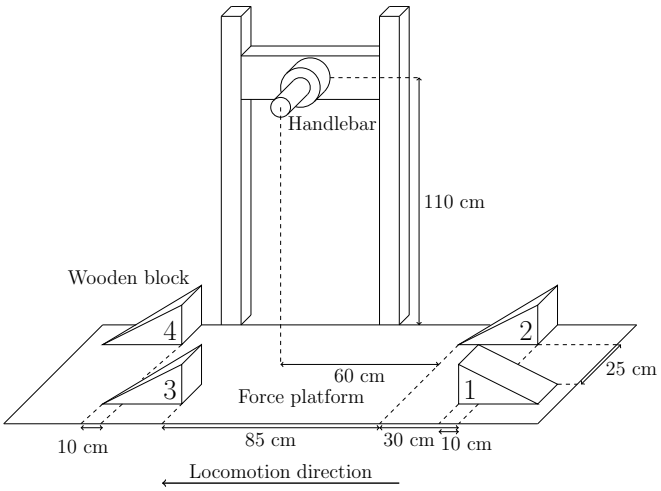

Fig. 2: Schema of the experimental setup with the range of distances considered. The scenario is composed of four tilted and adjustable wooden blocks. Each wooden block is topped with an adherent layer to prevent subjects from slipping.

When $\lambda = 0$, A is the projection of B onto Δ. In particular, $d_{G-\Delta}$ is:

$$d_{G-\Delta} = \frac{||\mathbf{f} \times \mathbf{m_G}||}{||\mathbf{f}||^2} = \frac{||\dot{\mathbf{h}}_\mathbf{G}|| \cdot |\sin(\theta)|}{||\mathbf{f}||} \tag{4}$$

where $\dot{\mathbf{h}}_\mathbf{G} = \mathbf{m_G}$ is the derivative of the angular momentum expressed at G and θ is the angle between $\mathbf{f}$ and $\dot{\mathbf{h}}_\mathbf{G}$. Hence, minimizing this distance amounts to minimize either the derivative of angular momentum at G, or the cosine angle between the contact forces and the derivative of the angular momentum at G, or to increase the norm of contact forces. This will be discussed later on.

III. Experimental validation of the criterion

In the following, we describe the experimental protocol we used to to measure $d_{G-\Delta}$ under increasingly destabilizing locomotion tasks for humans.

A. Participants

Fifteen healthy male subjects (25.6 $\pm$ 5.8 y, height 1.77 $\pm$ .035 m, body mass 73 $\pm$ 8 kg) volunteered for this investigation. The participants had no prior or existing injury or neurological disorder affecting gait. Each participant was informed of the experimental procedure and signed an informed consent form prior to the study. The experiment was conducted in accordance with the declaration of Helsinki (rev. 2013) with formal approval of the ethics evaluation committee (IRB00003888, Opinion number 13-124) of the Institut National de la Santé Et de la Recherche Médicale, INSERM, Paris, France.

B. Experimental protocol

Each participant had to execute different barefoot walking tasks under different stepping conditions and involving an additional hand contact or not (Fig. 1). They performed three trials in five different experimental conditions. For

Task	Standard walking	Walking on setup		Walking on setup using handlebar	
Speed	Spontaneous	Spontaneous	Fast	Spontaneous	Fast
Condition	A	B	D	C	E
$d_{G-\Delta}$ (mm)	55.1 ± 6.2	$(74.8 \pm 14.2)^{\star}$	150.9 ± 34.4	69.6 ± 13.5	123.8 ± 25.1
Average speed $(m.s^{-1})$	1.0 ± 0.15	$(0.71 \pm 0.24)^{\star}$	$(1.4 \pm 0.35)^{\dagger}$	0.73 ± 0.21	1.5 ± 0.32

TABLE I: Distances between the central axis of the external contact wrench and G, and average locomotion speeds across conditions A, B, C, D and E. Data are expressed as mean $\pm$ SD. Superscript $\star$ (resp. $\dagger$) stands for "Not significantly different from conditions C (resp. E)".

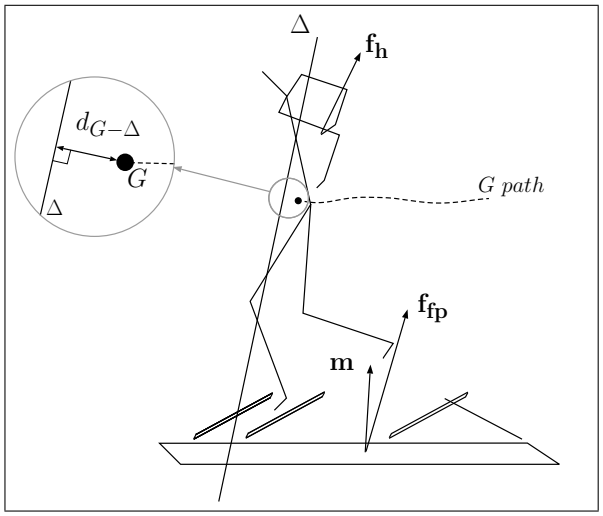

Fig. 3: Data reconstruction. $\mathbf{f_{fp}}$ is the force recorded from the force platform, $\mathbf{f_h}$ is the force recorded from the handlebar, $\mathbf{m}$ is the global moment expressed at the center of the force platform. Δ is the central axis of the external contact wrench. The dashed curved line is the path of G in time. The skeleton is displayed by linking the center-of-mass positions of each segment. $d_{G-\Delta}$ is highlighted in the magnified portion of the image.

each condition, two preliminary steps were achieved before crossing the force platform. Time intervals of about 3 minutes were adjusted to prevent fatigue between repetitions. For conditions involving non-coplanar contacts to be achieved, a custom made setup was built which consisted of four 35° sloped wooden blocks (i.e. three steps) fixed on the force platform embedded into the floor. A 6-component force sensor, hereafter called handlebar, was placed at 1.1 m high between blocks 2 and 3, which led to the wider step (see details Fig. 2).

In the first condition (condition A), the volunteers were asked to walk through the horizontal force platform, at spontaneous speed without any obstacle.

After warming-up and getting familiarized with the setup, the participants were asked to cross the platform (left foot first), walking on the experimental setup for the four remaining conditions:

- B, at spontaneous speed, without handlebar
- C, at spontaneous speed, using the handlebar
- D, as fast as possible, without handlebar
- E, as fast as possible, using the handlebar

For conditions B, C, D and E, subjects were asked to cross the platform walking on the wooden blocks only, which were spaced in order to disturb locomotion (Tab. I). There was no randomization but the volunteers were asked to perform the tasks in order of increasing complexity (conditions A, C, B, E then D). The protocol was not normalized to participants' specific attributes (size, weight, handedness), because the aim of the study was not to measure some absolute values of $d_{G-\Delta}$ under specific constraints but rather to compare relative results under different stability conditions.

C. Data acquisition

For 3-dimensional kinematic analysis, 47 reflective markers were fixed on the subject's bone landmarks for local frame reconstruction according to [13]. Data were recorded by thirteen optoelectronic cameras sampled at 200 Hz. The 6-dimensional external contact wrench applied to the subject was provided by the force platform and the handlebar, both sampled at 2 kHz. The handlebar was localized thanks to 3D reflective markers. Data were synchronized using Nexus 1.7.1 and filtered using a 4th order, zero phase-shift, low-pass Butterworth with a 15 Hz cutoff frequency. Body segments masses and center of mass positions were calculated in accordance with anthropometric tables [14]. The acquisition procedure started when the right foot of the subject left the floor and stopped before the left foot reached the floor, in order to record full contact motions. A custom made program was written for data processing (Fig. 3).

D. Statistics

The average $d_{G-\Delta}$ was computed for each subject under each condition. Before statistical tests, data normality was assessed using the Kolmogorov-Smirnov's test. Two separate one-way repeated measure ANOVAs were performed to compare the mean distance and the locomotion speed across conditions ($p < 0.001$) each followed by ten paired t-tests with the Bonferroni correction ($p < 0.05/10$) to assess the effect of each condition on $d_{G-\Delta}$ and to verify if speed instructions significantly modified subjects locomotion speed. The main hypothesis was accepted if the mean of $d_{G-\Delta}$ significantly increased as the stability of the subject was put at risk, by order of increasing destabilization : conditions A, C, B, E then D.

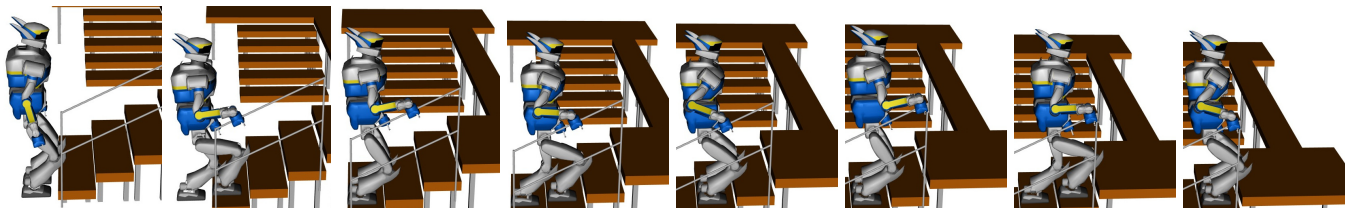

Fig. 4: Snapshots of the 15-cm steps climbing motion with handrail by the HRP-2 robot in simulation.

E. Experimental results

Locomotion velocity and $d_{G-\Delta}$ are shown in Tab. I. Our results reveal that subject's locomotion in conditions B and C is significantly slower than in conditions A, D and E (about twice), and it is significantly faster in conditions D and E than in condition A. This shows that participants well observed speed instructions. Paired t-tests reveal that $d_{G-\Delta}$ in B tested against C cannot be said to be significantly different (Tab. I). Every other figure in Tab. I shows that the mean distance significantly increases across the different conditions (ranging from 55.1 mm to 150.9 mm, by order of increasing distance : A,C-B,E then D).

F. Discussion

One first result of this study is that, compared to standard locomotion on level ground, asking the subject to walk on the destabilizing setup noticeably increases $d_{G-\Delta}$ (condition A against B, C, D and E). In [15] and [16], the authors suggest that holding a fixed element during locomotion or stair ascent and descent slightly improves stability and balance confidence. Although we cannot say if, at spontaneous speed, using the handlebar modifies the distance $d_{G-\Delta}$ or not, in this study, at high speed, when subjects are allowed to stabilize themselves using the handlebar (condition E), the distance significantly decreases in comparison with the corresponding condition at the same speed but without the handlebar (condition D). Statistical results show that participants well observe speed instructions. When they are asked to cross the platform at high speed (conditions D and E), $d_{G-\Delta}$ increases in comparison with the corresponding conditions at spontaneous speed (conditions B and C). In [17] and [18], the authors have shown that in young and older adults, dynamic stability can be improved by walking slower and therefore speed is a destabilizing parameter. The present study shows that $d_{G-\Delta}$ significantly increases with locomotion speed.

Looking into the three different parameters used to perturb the locomotion of the volunteers we observe that $d_{G-\Delta}$ increases with the difficulty of the task. One can sum up these results as follow : the more stable, the closer the CoM to Δ.

In this study, we first theoretically showed that lowering $d_{G-\Delta}$ contributes to the minimization of the variation of angular momentum expressed at the center of mass. On account of this mechanical argument we have measured $d_{G-\Delta}$ during experimental walking tests in destabilizing conditions. Based on this observation we claim that $d_{G-\Delta}$ could constitute a key element in the study of human locomotion stability. The angular momentum has already been widely studied to quantify locomotion stability [19] and it was suggested that it could be regulated by the central nervous system via the control of the position of the center of mass and the ground reaction forces [20]. However, our criterion is more versatile than only controlling the angular momentum, since one has more options to regulate it (Eq. (4)). Moreover, it reduces to the computation of a distance which makes it simple and expressive at the same time. It is worth mentioning that our study relies on the accuracy of markers placement to estimate segments centers of rotation and on anthropometric tables which are not fitted to each subject, resulting in an estimation error for the position of the center of mass [21], [22]. This error is increased by soft tissue artifacts [23]. A limitation of the proposed criterion is that, as soon as contacts are lost (dynamic jumping motions), the measured distance is zero (which is consistent with the conservation of angular momentum), and that indicates a stable motion whatever is happening in the air. Another drawback of this work lies in the fact that it needs full body motion capture to be recorded, whereas other criteria such as CoP only need forces and moments applied to the subject to be recorded. In the context of humanoid robotics however, this criterion can easily be used as a regulated cost for humanoid trajectory generation. This is what is presented in the next section.

IV. Humanoid robot trajectory generation

In this section, we implement the minimization of $d_{G-\Delta}$ in the context of multi-contact locomotion for the humanoid robot HRP-2. In order to highlight the efficiency of our criterion on real applications, we apply it on a stair climbing scenario where the robot has to use the handrail for helping itself.

A. General overview of the generation pipeline

The pipeline used is the same as the one originally introduced in [7] and recently extended in [24] and [10]. This formulation allows to compute a feasible trajectory (both kinematically and dynamically feasible) for the centroidal dynamics according to a sequence of contacts given as input. As a reminder, the centroidal dynamics is the dynamics of the whole-body system projected at its CoM. From the sequence of contacts and the centroidal dynamics trajectory, we use an inverse dynamics solver [25] to compute the whole-body

motion. Currently, all the trajectories of the end-effectors are designed by hand.

B. Centroidal optimal control formulation

The central piece of this pipeline is the module for generating centroidal trajectories. To be effective, these centroidal trajectories must be dynamically consistent, i.e., all the contact forces which drive the centroid must lie inside the friction cones. In addition, these trajectories must be kinematically feasible by the whole-body model. For instance, the CoM trajectory computed by the module must be achievable by the whole body when computing its inverse dynamics.

To solve this problem, we set up a multi-stage optimal control problem over a sequence of contacts S of the following form:

$$\min_{\underline{\boldsymbol{x}},\underline{\boldsymbol{u}},(\Delta t_s)} \quad \sum_{s=1}^{S} \int_{t_s}^{t_s+\Delta t_s} \ell_s(\boldsymbol{x},\boldsymbol{u}) - \log \underbrace{\mu_s(\boldsymbol{x},\boldsymbol{u})}_{\text{feasibility measure}} \quad dt \tag{5a}$$

$$\text{s.t.} \quad \forall t \quad \dot{\boldsymbol{x}} = f(\boldsymbol{x},\boldsymbol{u}) \tag{5b}$$

$$\forall t \quad \boldsymbol{u} \in \mathcal{K} \tag{5c}$$

$$\boldsymbol{x}(0) = \boldsymbol{x}_0 \tag{5d}$$

$$\boldsymbol{x}(T) = (\boldsymbol{c}_f, \boldsymbol{0}, \boldsymbol{0}), \dot{\boldsymbol{x}}(T) = \boldsymbol{0} \tag{5e}$$

where (5a) is the cost function we aim to minimize that contains a feasibility measure to encode the constraints of the centroidal dynamics w.r.t. the whole-body [10], [24]. It also handles a taylored cost function ℓ_s that can be adjusted by the user to obtain smoother motions for instance, or to penalize some quantities. Eq. (5b) is the centroidal dynamics of the system with state $\boldsymbol{x} = (\boldsymbol{c}, m\dot{\boldsymbol{c}}, \boldsymbol{h}_G)$ composed of G position vector ($\boldsymbol{c}$), the linear momentum and the angular momentum. The control $\boldsymbol{u}$ is the external contact wrench. To be effective, this external contact wrench must remain inside a certain cone called the centroidal wrench cone expressed in (5c) and introduced in [9]. In [10], the authors suggest an efficient inner approximation of this cone that we use in this work. Finally, starting from an initial state (5d), we want to reach a final state at rest, encoded by Eq. (5e). In this implementation, the duration of each phase is left as a free variable Δt_s of the problem. To solve this optimal control problem, we use MUSCOD-II [26], a multiple-shooting framework dedicated to problems having a shape similar to (5). In order to show the performances of our criterion, we provide the OCP solver with different cost functions ℓ_s:

1) in the first case, we investigate the minimization of the distance $d_{G-\Delta}$. In addition, we try to minimize the kinetic energy of the system in translation. Thus, we aim at minimizing $\ell_s = d_{G-\Delta} + \alpha\, m\|\dot{\boldsymbol{c}}\|^2$ where α is a weight between the two cost terms in ℓ_s;
2) in the second case, we let the angular momentum free and the cost function is only composed of the kinetic term leading to $\ell_s = m\|\dot{\boldsymbol{c}}\|^2$.

C. Simulation results

The simulated environment is an industrial stairway made of four 15-cm high steps and equipped with a handrail. The steps have a length of 30 cm. The complete motion, result of the simulation, is depicted in Fig. 4.

In Fig. 5 we display $d_{G-\Delta}$ for the two cases of study. When $d_{G-\Delta}$ is included in the cost function, it is successfully regulated to nearly zero during the whole motion.

In Fig. 6, we display the control input that drives the centroidal dynamics in the two approaches. As a result of the solved OCP, when our criterion is added to the cost function, the derivative of angular momentum about x and y axes is nearly zero. Reaction forces being mostly vertical in this kind of motion, the fact that the z component of angular momentum variation is not zero is consistent with Eq. (4) and with the fact that $d_{G-\Delta}$ is regulated to almost zero. Furthermore, one can notice that minimizing our criterion leads to greater accelerations of the CoM. This could be the result of a tighter control needed on the position of the CoM for regulating $d_{G-\Delta}$ to zero.

In Fig. 7, we display the state of the centroidal dynamics for the two cases of study. Noticeably, including our criterion in the cost function results in a nearly zero angular momentum about x and y axes which is a expected outcome of the computed optimal control.

D. Discussion

As mentioned earlier, minimizing $d_{G-\Delta}$ inside the cost function amounts to minimize either $\dot{\boldsymbol{h}}_G$ or the angle between $\boldsymbol{f}_c$ and $\dot{\boldsymbol{h}}_G$ or to maximize $||\boldsymbol{f}_c||$ (see Eq. (4)). This last strategy cannot be found by the solver since we also penalize the kinetic energy of the system in translation, which is equivalent to bound the variations of the linear acceleration of the centroidal dynamics [27].

Simulation results show that in the context of stair climbing, the solution found by the OC framework is noticeably the same as if the criterion was to minimize $\dot{\boldsymbol{h}}_G$. Normally, this strategy is either strictly imposed by the cart table model in [2], or minimized inside the cost function in [6] for instance. But given the different available strategies to change $d_{G-\Delta}$, we claim that our criterion allows for more slackness in the resolution of the problem (e.g. with a non zero components of $\dot{\boldsymbol{h}}_G$ along the direction of $\boldsymbol{f}_c$ when necessary). Thus, one could extend the minimization of this cost function to state-of-the-art motions in humanoid robotics that involves the contribution of all the limbs in the production of angular momentum.

We can also argue that regulating the angular momentum quantity to zero in the locomotion of biped robots is an arbitrary choice. A priori, it simplifies the control strategy of the whole body but may lead to a certain conservatism. Indeed, some locomotion tasks may require a non-negligible angular momentum quantity for maintaining balance of the robot, like for push recovery for instance or just walking on uneven surfaces [28].

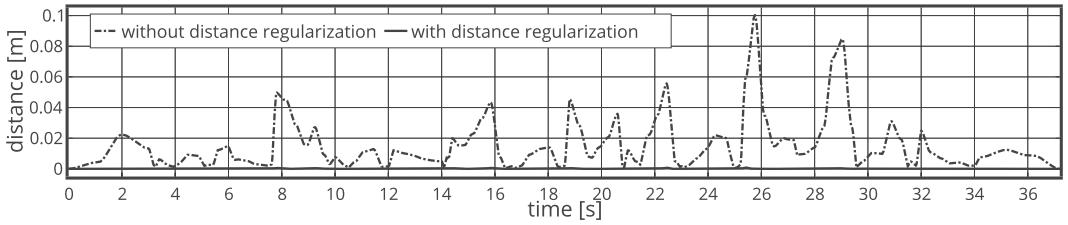

Fig. 5: Traces representing the distance $d_{G-\Delta}$ in the two cases of study: with and without regularization of $d_{G-\Delta}$.

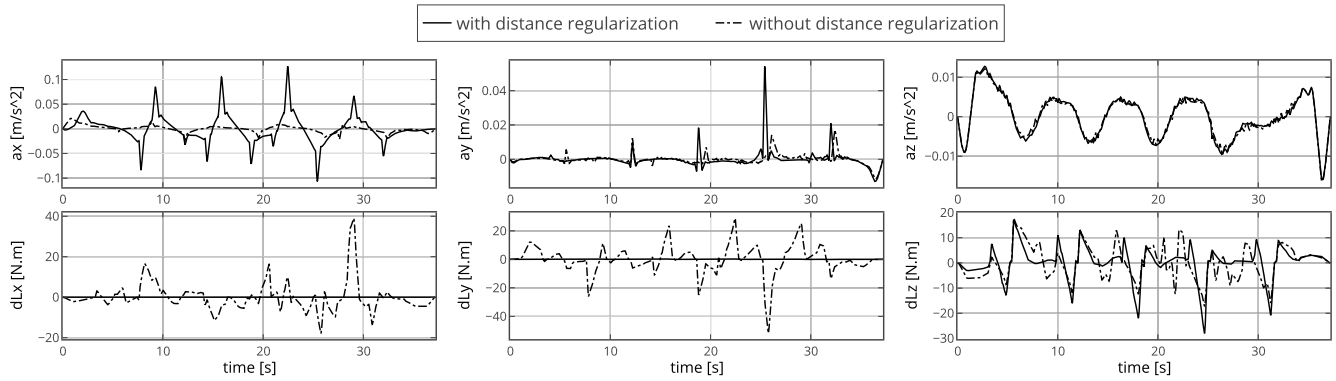

Fig. 6: Traces representing the control input (acceleration of the CoM and the angular momentum variations expressed around the CoM) that drives the centroidal dynamics in the two cases of study: with and without regularization of $d_{G-\Delta}$.

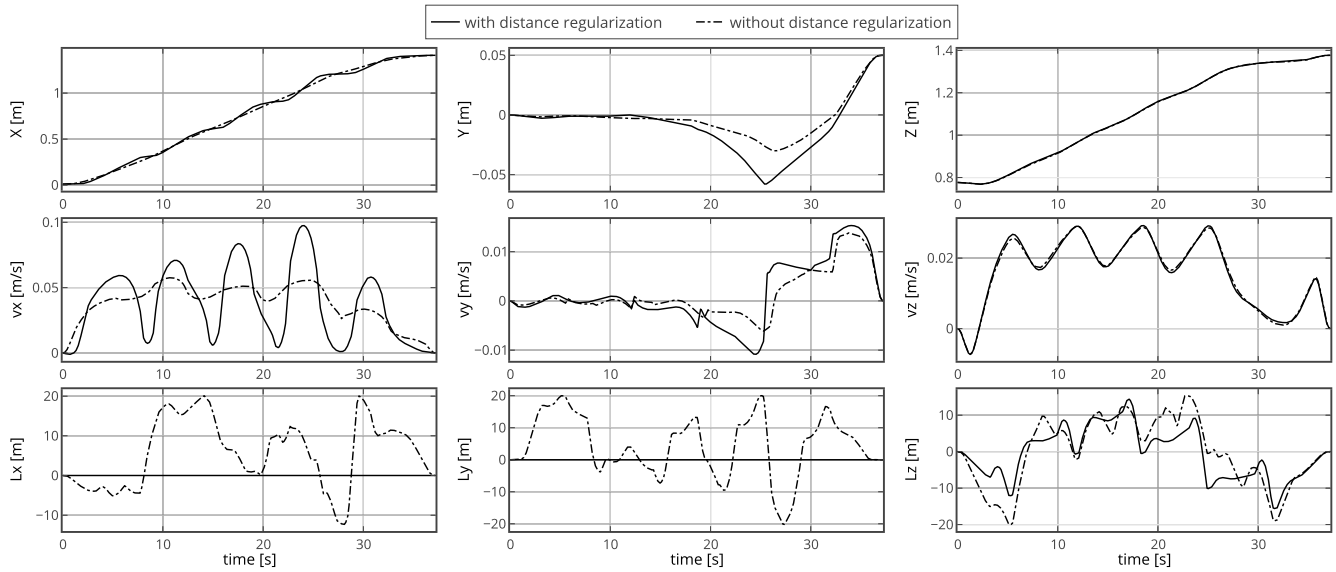

Fig. 7: Traces representing trajectories of the state of the centroidal dynamics in the two cases of study: with and without regularization of $d_{G-\Delta}$.

V. Conclusion

In this work we have proposed a new mechanical criterion for studying human locomotion stability, which is plausibly controlled by the CNS ([20], [29]): $d_{g-\Delta}$. We have measured significant variations of this distance in humans, correlated to the difficulty of the locomotion tasks specifically designed for this purpose. Then we have integrated this criterion in an optimal control framework for humanoid robots trajectory generation in a multi contact scenario. We have shown that its minimization allows for generating human like trajectories, in a same manner as minimizing angular momentum derivative but with more versatility since our criterion could generalize to more complex scenarios. This makes our approach a compact formulation of a versatile locomotion strategy for regulating the derivative of angular momentum, in order to prevent bipedal systems from tipping over.

ACKNOWLEDGMENT

We thank the volunteers who took part in the experiment. We warmly thank Dr. Robin Baurès, associate professor at the University of Toulouse for helping us with the statistics. This work is supported by the European Research Council through the Actanthrope project (ERC Grant Agreement 340050), the RoboCom++ FLAG-ERA JTC 2016 proposal and the French National Research Agency project Loco3D (ANR Grand Agreement ANR-16-CE33-0003).

REFERENCES

[1] P. Sardain and G. Bessonnet, "Forces acting on a biped robot. center of pressure-zero moment point," *Trans. Sys. Man Cyber. Part A*, 2004. [Online]. Available: http://dx.doi.org/10.1109/TSMCA.2004.832811

[2] S. Kajita, H. Hirukawa, K. Harada, and K. Yokoi, *Introduction to Humanoid Robotics*, ser. Springer Tracts in Advanced Robotics. Springer Berlin Heidelberg, 2014. [Online]. Available: https://books.google.fr/books?id=guIkBAAAQBAJ

[3] G. R. Fernie, C. I. Gryfe, P. J. Holliday, and A. Llewellyn, "The relationship of postural sway in standing to the incindence of falls in geriatric subjects," *Age and Ageing*, 1982.

[4] J. J. Collins and C. J. De Luca, "Open-loop and closed-loop control of posture: a random-walk analysis of center-of-pressure trajectories," *Experimental brain research*, 1993.

[5] T. E. Prieto, J. B. Myklebust, R. G. Hoffmann, E. G. Lovett, and B. M. Myklebust, "Measures of postural steadiness: differences between healthy young and elderly adults," *IEEE Transactions on biomedical engineering*, 1996.

[6] H. Dai, A. Valenzuela, and R. Tedrake, "Whole-body motion planning with centroidal dynamics and full kinematics," in *IEEE-RAS Int. Conf. on Humanoid Robotics (ICHR)*, 2014.

[7] J. Carpentier, S. Tonneau, M. Naveau, O. Stasse, and N. Mansard, "A versatile and efficient pattern generator for generalized legged locomotion," in *IEEE-RAS Int. Conf. on Robotics and Automation (ICRA)*, 2016.

[8] K. Harada, S. Kajita, K. Kaneko, and H. Hirukawa, "Zmp analysis for arm/leg coordination," in *IEEE/RSJ Int. Conf. on Intelligent Robots and Systems (IROS)*, Oct 2003.

[9] H. Hirukawa, H. Shizuko, K. Harada, S. Kajita, K. Kaneko, F. Kanehiro, K. Fujiwara, and M. Morisawa, "A universal stability criterion of the foot contact of legged robots - adios zmp," in *IEEE-RAS Int. Conf. on Robotics and Automation (ICRA)*, 2006.

[10] J. Carpentier and N. Mansard, "Multi-contact locomotion of legged robots," *Submitted to IEEE Transactions on Robotics (TRO)*, 2017.

[11] F. M. Dimentberg, "The screw calculus and its applications in mechanics," DTIC Document, Tech. Rep., 1968.

[12] T. Shimba, "An estimation of center of gravity from force platform data," *Journal of biomechanics*, 1984.

[13] G. Wu, F. C. Van der Helm, H. D. Veeger, M. Makhsous, P. Van Roy, C. Anglin, J. Nagels, A. R. Karduna, K. McQuade, X. Wang, *et al.*, "Isb recommendation on definitions of joint coordinate systems of various joints for the reporting of human joint motion—part ii: shoulder, elbow, wrist and hand," *Journal of biomechanics*, no. 5, pp. 981–992, 2005.

[14] R. Dumas, L. Cheze, and J.-P. Verriest, "Adjustments to McConville et al. and Young et al. body segment inertial parameters," *Journal of biomechanics*, 2007.

[15] E. V. Lamont and E. P. Zehr, "Earth-referenced handrail contact facilitates interlimb cutaneous reflexes during locomotion," *Journal of neurophysiology*, 2007.

[16] S. M. Reid, A. C. Novak, B. Brouwer, and P. A. Costigan, "Relationship between stair ambulation with and without a handrail and centre of pressure velocities during stair ascent and descent," *Gait & posture*, 2011.

[17] J. B. Dingwell and L. C. Marin, "Kinematic variability and local dynamic stability of upper body motions when walking at different speeds," *Journal of biomechanics*, 2006.

[18] H. G. Kang and J. B. Dingwell, "Effects of walking speed, strength and range of motion on gait stability in healthy older adults," *Journal of biomechanics*, 2008.

[19] M. Popovic, A. Hofmann, and H. Herr, "Angular momentum regulation during human walking: biomechanics and control," in *IEEE-RAS Int. Conf. on Robotics and Automation (ICRA)*, 2004.

[20] H. Herr and M. Popovic, "Angular momentum in human walking," *Journal of experimental biology*, 2008.

[21] G. Rao, D. Amarantini, E. Berton, and D. Favier, "Influence of body segments' parameters estimation models on inverse dynamics solutions during gait," *Journal of biomechanics*, 2006.

[22] J. Carpentier, M. Benallegue, N. Mansard, and J.-P. Laumond, "Center of Mass Estimation for Polyarticulated System in Contact — A Spectral Approach," *Transactions on Robotics (TRO)*, 2016.

[23] A. Peters, B. Galna, M. Sangeux, M. Morris, and R. Baker, "Quantification of soft tissue artifact in lower limb human motion analysis: a systematic review," *Gait & posture*, 2010.

[24] J. Carpentier, R. Budhiraja, and N. Mansard, "Learning feasibility constraints for multi-contact locomotion of legged robots," in *Robotics: Science and System (RSS)*, 2017.

[25] L. Saab, O. E. Ramos, F. Keith, N. Mansard, P. Soueres, and J.-Y. Fourquet, "Dynamic whole-body motion generation under rigid contacts and other unilateral constraints," *Transactions on Robotics (TRO)*, 2013.

[26] D. Leineweber, I. Bauer, H. G. Bock, and J. P. Schlöder, "An efficient multiple shooting based reduced sqp strategy for large-scale dynamic process optimization. part 1: theoretical aspects," *Computers & Chemical Engineering*, 2003.

[27] P.-B. Wieber, "Viability and predictive control for safe locomotion," in *IEEE/RSJ Int. Conf. on Intelligent Robots and Systems (IROS)*, 2008.

[28] A. Herzog, S. Schaal, and L. Righetti, "Structured contact force optimization for kino-dynamic motion generation," in *IEEE/RSJ Int. Conf. on Intelligent Robots and Systems (IROS)*, 2016.

[29] R. R. Neptune and C. P. McGowan, "Muscle contributions to whole-body sagittal plane angular momentum during walking," *Journal of biomechanics*, 2011.